Tour example where the neglected effects of the disturbing acceleration due to other planets proved significant. Errors in final position for numerical integration of individual legs using the calculated initial velocity range from 1.6 km to 240,000 km with the bulk of the values in the 2–2000 km interval.

References

[1] Bayliss, S. S., "Precision Targeting for Multiple Swingby Interplanetary Trajectories," TE-39, June 1970, Measurement Systems Lab., MIT, Cambridge, Mass.

[2] Silver, B., "Grand Tours of the Jovian Planets," *Journal of Spacecraft and Rockets*, Vol. 5, No. 6, June 1968, pp. 633–637.

[3] Vanderveen, A., "Triple Planet Ballistic Flybys of Mars and Venus," *Journal of Spacecraft and Rockets*, Vol. 6, No. 4, April 1969, pp. 383–389.

[4] Sturms, F., "Trajectory Analysis of an Earth-Venus-Mercury Mission in 1973," TR-32-1062, Jan. 1967, Jet Propulsion Lab., Pasadena, Calif.

[5] Battin, R., *Astronautical Guidance*, McGraw-Hill, New York, 1964, pp. 75–82, 169–171.

[6] Carson, N., "An Explicit Analytic Guidance Formulation for Many-Body Space Trajectories," TE-30, May, 1969, Measurement Systems Lab., MIT, Cambridge, Mass., pp. 90.

[7] Bryson, A. and Ho, Y., *Applied Optimal Control*, Blaisdell, Waltham, Mass., 1969, pp. 19–21.

[8] Hildebrand, F., *Introduction to Numerical Analysis*, McGraw-Hill, New York, 1956, pp. 447–451.

[9] Goodyear, W., "A General Method for the Computation of Cartesian Coordinates and Partial Derivatives of the Two-Body Problem," CR-522, Sept. 1966, NASA.

SEPTEMBER 1971 J. SPACECRAFT VOL. 8, NO. 9

Analysis of Mariner VII Pre-Encounter Anomaly

H. J. GORDON,* S. K. WONG,† AND V. J. ONDRASIK‡
Jet Propulsion Laboratory, Pasadena, Calif.

The loss of signal at 127 hr before closest approach to Mars and the subsequent changes in the spacecraft and in its trajectory are described. Real-time orbit determination activity as well as postencounter analysis are discussed. Great difficulty was experienced in processing tracking data influenced by an unknown nongravitational force that could not be properly modeled. Results of simulations using known perturbations are presented. It is concluded that the battery case had ruptured and vented into the interior of the spacecraft. This rupture caused corona discharges, and escaping gas produced the translational forces.

Introduction

AT 127 hr before Mariner VII was scheduled to encounter Mars, its radio signal was lost abruptly. When the signal was reacquired after 7 hr and 12 min, the doppler tone showed that the radial velocity had decreased by 1.89 cm/sec. There was no further change in velocity for 71 min, at which time two-way lock was lost again for 60 min; when reacquired, it showed that the radial velocity had decreased by an additional 0.78 cm/sec. The radial velocity continued to decrease at an apparently exponentially decaying rate during the next two weeks. This meant that the orbit had to be redetermined in less than five days (in the presence of a nongravitational force that was not modeled in the orbit determination programs) so that all science instruments could be optimally pointed during the encounter.

Orbit Determination

Orbit determination is done by an iterative, weighted, least-squares method that assumes Gaussian random errors superimposed on the tracking data as well as on the initial estimates. Reference 1 describes the basic concepts; Ref. 2 describes the single precision orbit determination program. (A double precision orbit determination program, DPODP, was constructed and used for the first time during the Mariner 69 operations.) The common types of data and their associated accuracies are shown in Table 1 and more fully described in Ref. 3.

A linearized coordinate system has been adopted to express the terminal coordinates of an interplanetary trajectory. This coordinate system, as described by Kizner,[4] is illustrated in Fig. 1. The terminal coordinates can be defined as $\mathbf{B}\cdot\mathbf{R}$ and $\mathbf{B}\cdot\mathbf{T}$ or as B and θ, where θ is the angle measured clockwise from $\mathbf{T}$ to $\mathbf{B}$ with the time of closest approach (T_{CA}).

Pre-Anomaly Orbits

Figure 2 shows the results of processing different lengths of data arcs, using different data types (doppler only or doppler plus range), and estimating different sets of parameters. The $\mathbf{B}\cdot\mathbf{R}$ and $\mathbf{B}\cdot\mathbf{T}$ coordinates are plotted, and the tight clus-

Table 1 Data types and accuracies

Data type	Measurement accuracy (1σ)	Comments
Two-way doppler	0.01 Hz = 0.7 mm/sec	Measures radial velocity
Three-way doppler	0.01 Hz = 0.7 mm/sec	Bias is typically 0.2 Hz
Mar IA range	35 m	Ground and spacecraft delay contribute
Planetary range	15 m	Ground and spacecraft delay contribute

Presented as Paper 70-1065 at the AAS/AIAA Astrodynamics Conference, Santa Barbara, Calif., August 19–21, 1970; submitted September 28, 1970; revision received March 26, 1971. This paper presents the results of one phase of research carried out at the Jet Propulsion Laboratory, California Institute of Technology, under Contract NAS 7-100, sponsored by NASA.

Index categories: Lunar and Planetary Trajectories; Spacecraft Navigation, Guidance and Flight-Path Control Systems.

* Member of the Technical Staff, Navigation and Mission Design Section, Jet Propulsion Laboratory, California Institute of Technology. Associate Fellow AIAA.

† Senior Research Engineer, Tracking and Orbit Determination Section.

‡ Senior Engineer, Tracking and Orbit Determination Section.

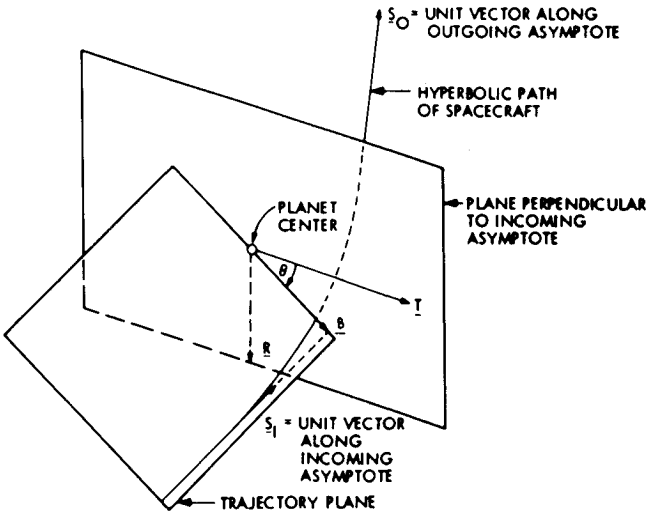

Fig. 1 *R, S, T* coordinate system.

ter of points indicates that the orbit determination process is converging.

Pre-Encounter Orbits

Figure 3 shows the doppler residuals just prior to and during the anomaly period. When convergence has been achieved, the residual should be essentially zero, as shown to the left side of Fig. 3. After the first Loss of Signal (LOS), residuals appear at a mean displacement of −0.29 Hz and are steady. After the second LOS, residuals are seen to be continuously decreasing; this indicates that a nongravitational force was being exerted. At the time, the form of this small force was not understood, though the residuals suggested an exponentially decaying model. (Such a model has been developed for the double precision orbit determination program, but was not available in August 1969.) The models that were built into the orbit determination program are as follows: 1) Attitude control jet model—solves for a constant force that may be turned on and off at selected times. These forces are considered to be along the spacecraft pitch, yaw, and roll axes so that any direction can be synthesized by an appropriate combination. 2) Solar pressure model—solves for a force that varies inversely as the square of the distance from the sun. These forces are considered to act in the radial direction from the sun, in the tangential direction that is in the trajectory

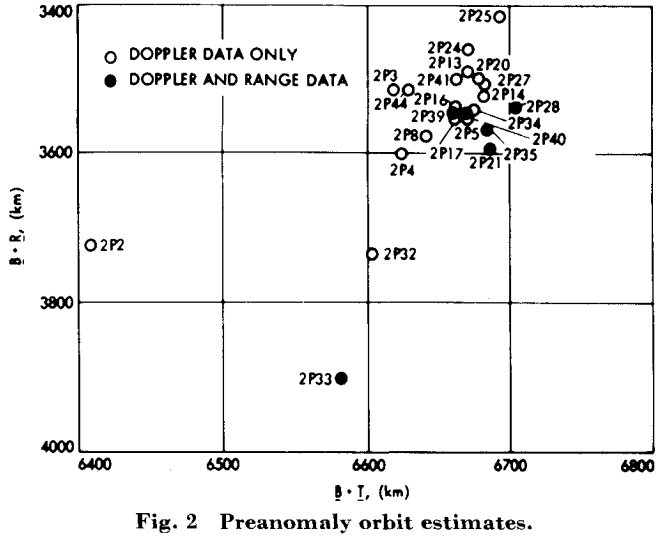

Fig. 2 Preanomaly orbit estimates.

Table 2 Effects of perturbing accelerations[a]

Description	ΔB, km[b]	$\Delta\mathbf{B}\cdot\mathbf{R}$, km[b]	$\Delta\mathbf{B}\cdot\mathbf{T}$, km[b]	ΔT_{CA}, sec[b]
$\Delta\bar{r}$ in r direction	−13.3	3.4	−16.5	−6.0
$\Delta\bar{r}$ in x direction	12.6	−30.6	29.0	−1.8
$\Delta\bar{r}$ in y direction	40.6	32.3	29.4	−0.7

[a] Perturbations start at encounter − 91 hr.
[b] ΔB = B(perturbed) − B(nominal), etc.

plane and perpendicular to the radial direction, and in the direction normal to the trajectory plane. 3) Motor burn model—solves for an impulsive velocity change at a given time. As many as three discrete burns may be modeled.

Clearly, none of these models apply properly to the observed effect. Each model was used, and the results are shown in Fig. 4. The effect of this small force, which could not be modeled correctly, was diminishing as a function of time. It was decided, therefore, to use very short data arcs§ of approximately 48 hr prior to the last data point for both the attitude control jet model and the solar pressure model. Finally, the sensitivity of instrument pointing to orbit determination errors was used to recommend an orbit on which to base the scan platform pointing angles so that minimum error would result. The actual orbit used for the final spacecraft platform update was $\mathbf{B}\cdot\mathbf{R}$ = 3650 km, $\mathbf{B}\cdot\mathbf{T}$ = 6725 km, and T_{CA} = 05:00:47.¶

Postencounter Orbits

After the successful encounter, additional tracking data were accumulated and used to refine the orbit. Data were accumulated for two days, up to the time of initiation of the infrared spectrometer cooldown. (A sophisticated cryogenic cooling system was used which vented N_2 and H_2 through a balanced tee, but still resulted in unbalanced forces of the order of several hundred dynes for a period of several hours.) The data were processed and the results were $\mathbf{B}\cdot\mathbf{R}$ = 3764 km, $\mathbf{B}\cdot\mathbf{T}$ = 6647 km, and T_{CA} = 05:00:50.

With an additional three days of postencounter data, the results were $\mathbf{B}\cdot\mathbf{R}$ = 3631 km, $\mathbf{B}\cdot\mathbf{T}$ = 6713 km, and T_{CA} = 05:00:50.

By a careful examination of the residuals from the postencounter fits, it was determined that the anomalous nongravitational force had become negligibly small by August 13

Analysis of Range Data

Range data were analyzed so that events during the first LOS could be evaluated. A basis for comparison was available, since the doppler measurements corresponded to range rate, and since the range itself was measured before and after the period of LOS. The last range measurement before the anomaly was taken at 7/28/69, 07:20:02, and the first range measurement after the anomaly was taken at 8/2/69, 03:12:02. The difference between the range residuals was −9209 ± 20 m. Therefore

$$\int_{t_0}^{t_5} \Delta\dot{R}dt = -9209 \pm 20 \text{ m}$$

as measured with the planetary ranging system.

The exact shape of the doppler residuals that would have existed is indeterminable, but some insight may be gained if it is assumed that a step function exists at some time after LOS, or that a ramp starts right at the LOS; Fig. 5 shows these two assumptions.

§ Data arc is a period of time during which data were obtained.
¶ Time of closest approach (T_{CA}) always refers to August 5, 1969.

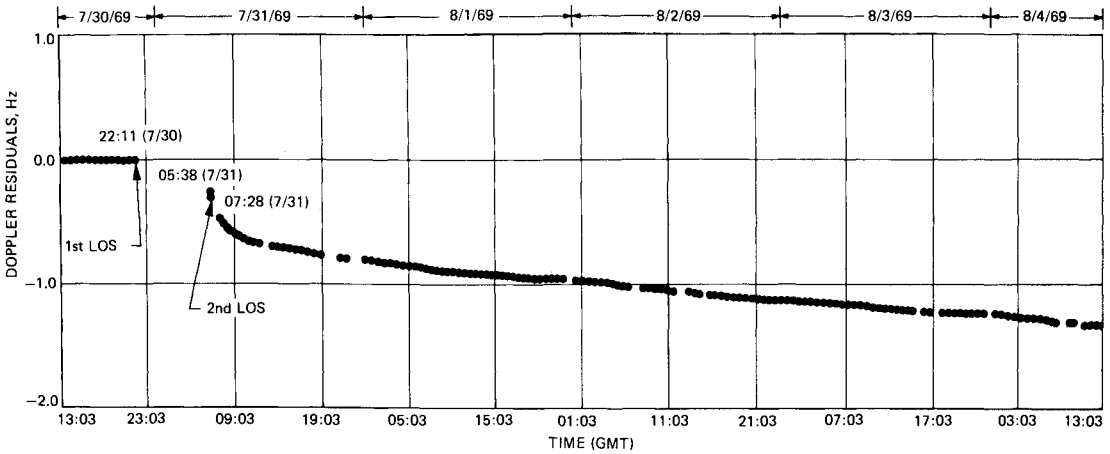

Fig. 3 Doppler residuals vs time near Mariner VII anomaly.

For the step function

$$\int_{t_0}^{t_5} \Delta\dot{R}dt = \int_{t_2}^{t_4} -1.89 \text{ cm/sec } dt + \int_{t_4}^{t_5} f(t)dt$$

which yields t_2 = 7/31/69, 00:13:00 ± 9 min, where: t_0 = time of last pre-anomaly range point − 7/28/69, 07:20:02; t_4 = time of last good doppler point before second LOS—7/31/69, 06:33:17; t_5 = time of first post-anomaly range point—8/2/69, 03:12:02; and $f(t)$ = polynomial curve fit to doppler residuals, (expressed in cm/sec) from the second reacquisition, extrapolated backward to the second LOS.

Therefore, a step function would have had to occur 121 ± 9 min after the first LOS.

For the ramp,

$$\int_{t_0}^{t_5} \Delta\dot{R}dt = \int_{t_0}^{t_3} -1.89 \text{ cm/sec}(t - t_1)/(t_3 - t_1)dt + \int_{t_3}^{t_4} -1.89 \text{ cm/sec } dt + \int_{t_4}^{t_5} f(t)dt$$

which yields t_3 = 7/31/69, 02:13:32 ± 18 min, where t_1 = time of last doppler point before first LOS—7/30/69, 22:11:32.

Therefore, a ramp would have had to terminate 242 ± 18 min after the first LOS.

These calculations show that the velocity changed during the early part of the time that the signal was lost, and had stopped changing long before the reacquisition of signal at 7/31/69, 05:22:17.

Analysis of Simulated Data

During the Mariner VII operations and the postencounter analysis, many strategies were employed to determine the orbit of the spacecraft under the influence of the unknown perturbation. To formulate a strategy for dealing with such perturbations and to obtain some idea of how well the orbit might be determined, simulated data were produced so that the actual trajectory was a known quantity.

The first block of simulated data consisted of two-way Doppler points and associated partial derivatives that were produced every 10 min starting on July 31 at 22 hr and continuing to August 16 (for a nominal orbit with no perturbations). To avoid simulating and fitting data for every perturbation to be studied, the following procedure was followed: 1) A simple trajectory run was made and the desired perturbation was applied, then perturbed values of the geocentric range were obtained. 2) Perturbed geocentric range

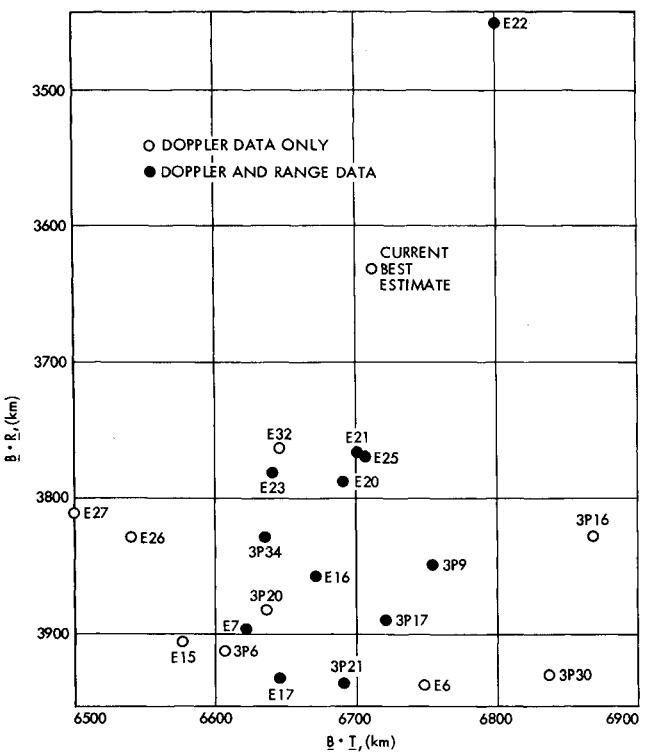

Fig. 4 Postanomaly orbit estimates.

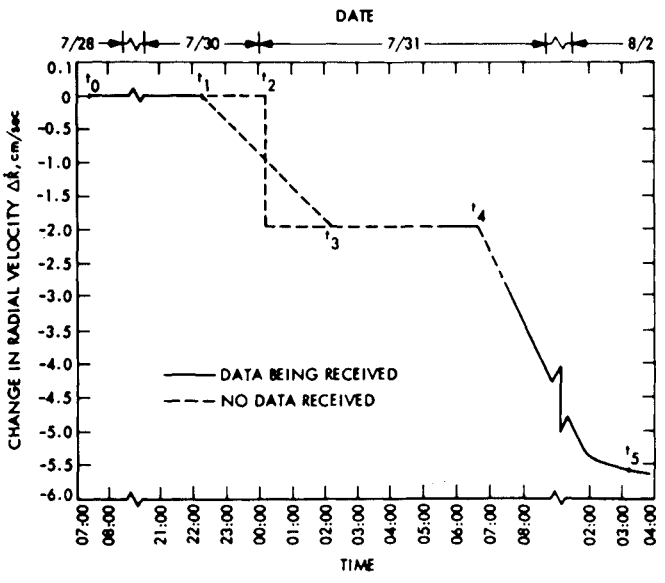

Fig. 5 Observed and modeled changes in radial velocity.

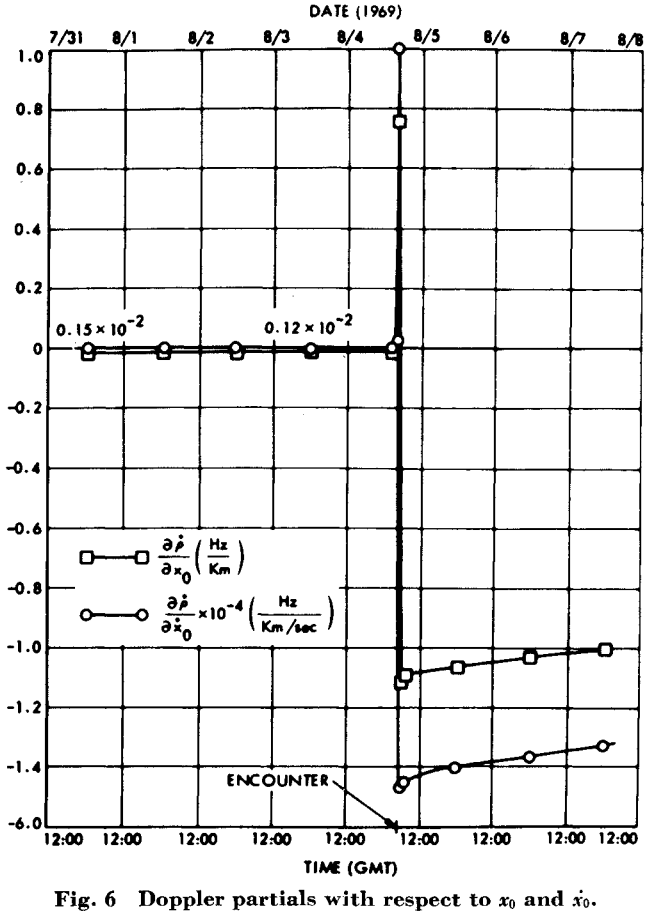

Fig. 6 Doppler partials with respect to x_0 and $\dot{x}_0$.

values were subtracted from the unperturbed values. 3) Range differences were used to produce the corresponding doppler differences with the program ION.[5] 4) Doppler differences were then treated as residuals in the nominal unperturbed run.

The effects of three perturbations were studied; namely, an exponential acceleration of magnitude $\Delta\ddot{r} = 0.26 \times 10^{-8}$ exp $(-t/18$ hr) km/sec^2 in the r, x, and y directions. (These directions correspond to the principal spacecraft axes: roll, pitch, and yaw, respectively.) This exponential form was chosen because it best approximated the actual acceleration experienced by Mariner VII. Table 2 shows the effect these accelerations had on the B-plane parameters.

Pre-Encounter Solutions

Figure 6 contains plots of the partial derivatives of the doppler data with respect to the x-components of geocentric position and velocity. (Partials with respect to y- and z-components are similar.) It is clear that the pre-encounter solutions, which could use data only up to encounter -4 hr, received very little help from the planet-centered accelerations in resolving uncertainties arising from the unmodeled forces.

Table 3 presents the results of orbit determination solutions obtained with various data arcs, and a priori statistics and estimated parameters, for exponential accelerations in the r, x, and y directions. This table substantiates the well-known fact that large unmodeled accelerations have disastrous effects upon the solution, and in this case may give errors in the encounter parameter of thousands of kilometers. An approximation to the change in the spherical coordinate state vector may be obtained by considering a first-order temporal expansion of the range rate given by the following equation[6]:

$$\dot{\rho}(t) = \dot{r} + \omega r_S \cos\delta(\sin\omega t + \Delta\lambda \cos\omega t) + [a_g + r(\dot{\alpha}^2 \cos^2\delta + \dot{\delta}^2)]t - r_S\omega t\dot{\delta} \sin\delta \sin\omega t - r_S\omega t\dot{\alpha} \cos\delta \cos\omega t \quad (1)$$

where $\dot{\rho}$ = topocentric range rate, $\dot{r}$ = geocentric range rate, δ = declination, α = right ascension, $\Delta\lambda$ = error in right ascension, r_S = distance of tracking station from spin axis of earth, a_g = gravitational acceleration, and $v_p = r(\dot{\alpha}^2 \cos^2\delta + \dot{\delta}^2)^{1/2}$ = velocity perpendicular to line of sight.

The orbit determination program will modify the elements r, $\dot{r}$, α, $\dot{\alpha}$, δ, and $\dot{\delta}$ to account for the unmodeled acceleration. For example, consider in a very simplified manner, the effects of a constant acceleration in the sun probe direction of magnitude 0.20×10^{-8} km/sec^2. The coefficients of the fourth term must rearrange themselves to account for this acceleration. Thus,

$$0.20 \times 10^{-8} \text{ km/sec}^2 = [\partial a_g/\partial r + (\dot{\alpha}^2 \cos^2\delta + \dot{\delta}^2)]\Delta r + \partial a_g/\partial\alpha\,\Delta\alpha + \partial a_g/\partial\delta\,\Delta\delta + 2v_p\Delta v_p/r \quad (2)$$

Table 3 Pre-encounter solutions for $\Delta\ddot{r} = 0.26 \times 10^{-8}$ exp$(-t/18$ hr$)^a$

Start of data arc[b]	Initial acceleration, km/sec^2	Direction of acceleration	Parameters estimated[c]	A priori standard deviations	$\Delta\mathbf{B}\cdot\mathbf{R}$, km[d]	$\Delta\mathbf{B}\cdot\mathbf{T}$, km[d]	ΔT_{CA}, sec[d]
E − 91 hr	0.26×10^{-8}	r	S	10^4 km, 1 km/sec	−10,111.6	682.7	93.5
E − 67 hr	0.065×10^{-8}	r	S	10^4 km, 1 km/sec	−1,762.5	58.1	3.6
E − 67 hr	0.065×10^{-8}	r	S, A in r only	100 km, 10 m/sec 10^{-6} km/sec^2 10^{-12} km/sec^3	181.7	343.9	−1.7
E − 30 hr	0.008×10^{-8}	r	S	1000 km, 10 m/sec	114.9	73.8	−1.3
E − 30 hr	0.008×10^{-8}	r	S, A, B	100 km, 1 m/sec 10^{-9} km/sec^2 10^{-14} km/sec^3	2.0	27.2	−0.9
E − 30 hr	0.008×10^{-8}	x	S	1000 km, 10 m/sec	−20.9	−1.1	−0.1
E − 30 hr	0.008×10^{-8}	x	S, A, B	100 km, 1 m/sec 10^{-9} km/sec^2 10^{-14} km/sec^3	39.3	27.8	−0.1
E − 30 hr	0.008×10^{-8}	y	S	1000 km, 10 m/sec	81.4	0.1	0.2
E − 30 hr	0.008×10^{-8}	y	S, A, B	100 km, 1 m/sec 10^{-9} km/sec^2 10^{-14} km/sec^3	−35.9	−9.4	0.2

[a] All data stops at encounter − 6 hr.
[b] E = encounter.
[c] S = state includes position and velocity components; acceleration is modeled: $\ddot{r} = A + Bt$, where A is constant and B is linear acceleration.
[d] $\Delta T_{CA} = T_{CA}$ from DPODP minus nominal T_{CA}, etc.

Table 4 Postencounter solutions for $\Delta\ddot{r} = 0.26 \times 10^{-8}$ exp$(-t/18$ hr$)$[a]

Perturbation direction	ΔB,[b] km	$\Delta\mathbf{B}\cdot\mathbf{R}$,[b] km	$\Delta\mathbf{B}\cdot\mathbf{T}$,[b] km	ΔT_{CA},[b] sec
r	−10.5	−0.1	−1.5	−1.1
x	4.3	10.5	−0.4	7.7
y	−1.2	25.2	−14.0	6.4

[a] Data were obtained between encounter − 103 hr and − 6 hr and between encounter + 9 hr and + 131 hr. Estimate state vector with a priori standard deviations of 10^{-4} km and 1 km/sec.
[b] $\Delta B = B$ from DPODP minus nominal B, etc.

The gravitational partials are so small that it would require changes in range of 0.2×10^6 km or changes in α or δ of approximately 1° to account for the unmodeled acceleration, gravitationally. These possibilities would be quite unreasonable and must be eliminated. In addition, the second or third choices are in conflict with the determination of α and δ from the second and third terms of Eq. (1). Thus, if it is assumed that the effects of the unmodeled accelerations will be absorbed in the perpendicular velocity, Eq. (2) yields

$$\Delta v_p = 0.20 \times 10^{-8} \text{ km}^2/\text{sec}^2/1.72 \times 10^{-7} \text{ km/sec} = 0.0116 \text{ km/sec}$$

This agrees well with the DPODP result of 0.0123 km/sec. Unfortunately, the correlation between the various coefficients of Eq. (1) prohibits such easy prediction of the changes in other quantities.

Table 3 also shows that the deletion of increasing amounts of data for which the exponential acceleration is large continually improves the "state-only" solution. Finally, with data accumulated during one day shortly before encounter, solutions are obtained with B-plane parameters that are usually within 40 km of the correct result and that have associated uncertainties of approximately 60 km. However, even with this data arc, the errors may sometimes be as large as 115 km. A comparison of the one-day data-arc, state-only solutions in Table 3 with perturbed minus nominal results in Table 2, indicates that errors in the solutions are almost always larger than actual differences in the perturbed and nominal trajectories. Thus, the effect of the unmodeled acceleration degrades the state-only solutions to such an extent that the use of these orbits would incur larger errors than the use of the nominal orbit that was determined before the acceleration is initiated.

The orbit solutions for the exponentially perturbed spacecraft are considerably improved if attitude control forces are included in the estimate list with the state parameters. For example, the errors in the 61-hr data-arc solutions, although still several hundreds of kilometers are improved by approximately a factor of five over the state-only solutions. The one-day data-arc solutions are improved to the point where the errors in the B-plane parameters are of the same size as the actual changes from the unperturbed trajectory.

Postencounter Solutions

Once the spacecraft has passed the planet so that both postencounter and pre-encounter data are available, the solution for the encounter parameters is greatly improved. Table 4 presents the results of using this pre- and post-encounter data for orbits produced by the exponential accelerations. It is seen that even the deletion of the data from encounter −6 hr to encounter +11 hr gives B-plane parameters which exceed 15 km only once. An order of magnitude prediction of the effect unmodeled accelerations have on the magnitude of B may be obtained as follows. Consider the spacecraft to be in a hyperbolic orbit about the encounter planet as shown in Fig. 7. The simplest situation to examine is that during which the perturbing acceleration is always directed toward the planet. For this case, the angular momentum per unit

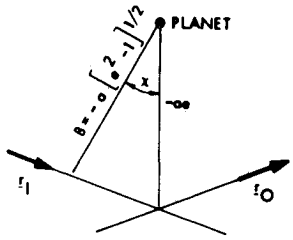

Fig. 7 Encounter hyperbola.

mass $h = B\dot{s}$ is conserved so that

$$\Delta B/B = -\Delta\dot{s}/\dot{s} \tag{3}$$

A state-only solution for the orbit perturbed by an exponential acceleration with the use of only pre-encounter data may give errors in the velocity up to 10^{-2} km/sec. By using this value for $\Delta\dot{s}$ in Eq. (3), one can predict an error of 10 km in B; this closely approximates the results in Table 4 which contains errors in B from 1 to 10 km.

If the perturbation is not in the spacecraft planet direction the situation is not so simple, but still tractable if some very reasonable assumptions are made. Again, consider the spacecraft to be in a hyperbolic orbit about the planet as shown in Fig. 7. From this figure, it is easily seen that $\cos\chi = (e^2 - 1)/e$ which, if expanded (and if terms of the order $1/e^2$ are neglected), becomes $\chi = 1/e$. The incoming and outgoing asympote unit vectors, $\mathbf{S}_I$ and $\mathbf{S}_O$, are given by $\mathbf{S}_I = \dot{\mathbf{r}}_I/\dot{s}$ and $\mathbf{S}_O = \dot{\mathbf{r}}_O/\dot{s}$ and the dot product between them may be written as

$$\mathbf{S}_I\cdot\mathbf{S}_O = \cos 2\chi = 1 - 2/e^2 \tag{4}$$

Thus, an error in the eccentricity is related to errors in velocity quantities by

$$\Delta e = -e^3/4[\mathbf{S}_O\cdot\Delta\dot{\mathbf{r}}_I/\dot{s} - 2\mathbf{S}_I\cdot\mathbf{S}_O\Delta\dot{s}/\dot{s} + \mathbf{S}_I\cdot\Delta\dot{\mathbf{r}}_O/\dot{s}] \tag{5}$$

since

$$\Delta\mathbf{S} = \Delta\dot{\mathbf{r}}/\dot{s} - \mathbf{S}\Delta\dot{s}/\dot{s} \tag{6}$$

For a two-body orbit the incoming and outgoing speeds must be the same so that $\Delta\dot{s}$, $\Delta\dot{\mathbf{r}}_I$, and $\Delta\dot{\mathbf{r}}_O$ must satisfy

$$\Delta\dot{s} = \mathbf{S}_I\cdot\Delta\dot{\mathbf{r}}_I = \mathbf{S}_O\cdot\Delta\dot{\mathbf{r}}_O$$

Thus, writing Eq. (5) as

$$\Delta e = -e^3/4[(\mathbf{S}_O - \mathbf{S}_I + \mathbf{S}_I)\cdot\Delta\dot{\mathbf{r}}_I + (\mathbf{S}_I - \mathbf{S}_O + \mathbf{S}_O)\cdot\Delta\dot{\mathbf{r}}_O - 2\mathbf{S}_I\cdot\mathbf{S}_O\Delta\dot{s}]$$

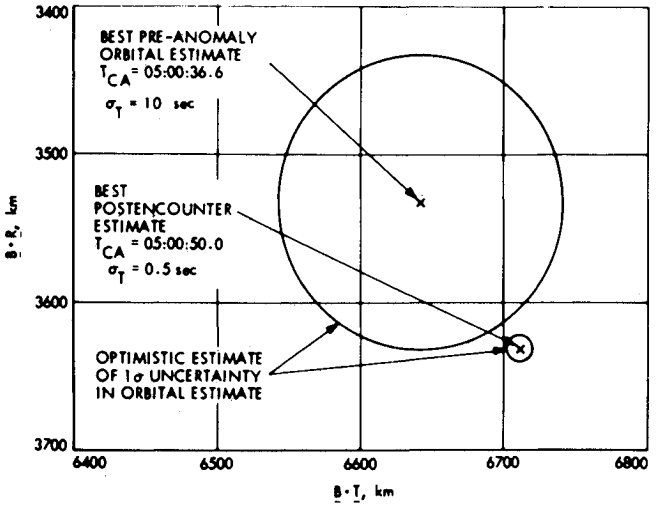

Fig. 8 Pre-anomaly and postencounter orbit determination estimates.

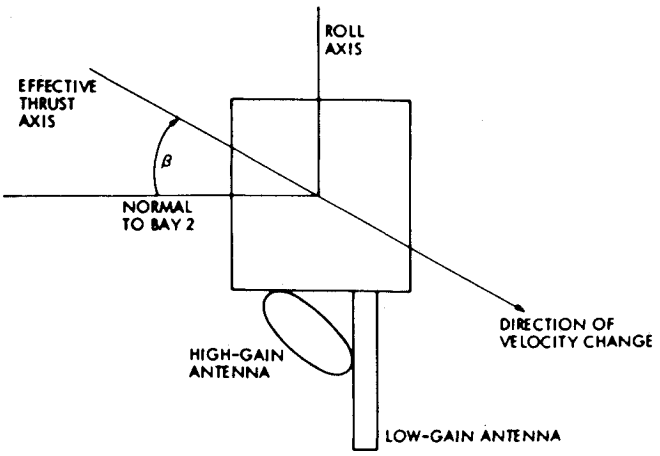

Fig. 9 Definition of thrust angle β.

and substituting in Eq. (6), one obtains

$$\Delta e = -e^3/4[(\mathbf{S}_O - \mathbf{S}_I)\cdot(\Delta\dot{\mathbf{r}}_I - \Delta\dot{\mathbf{r}}_O) + 2(1 - \mathbf{S}_I\cdot\mathbf{S}_O)\Delta\dot{s}] \quad (7)$$

From Eq. (4), it may be seen that $(1 - \mathbf{S}_I\cdot\mathbf{S}_O) = 2/e^2$ and $|(\mathbf{S}_O - \mathbf{S}_I)| = 2/e$. For any reasonable perturbative accelerations $|\Delta\dot{\mathbf{r}}_I - \Delta\dot{\mathbf{r}}_O| \propto 1/e\Delta\dot{s}$ and for convenience we will arbitrarily assume that the constant of proportionality equals two. Thus,

$$\Delta e \sim -2e\Delta\dot{s}/\dot{s} \quad (8)$$

The eccentricity may also be written in terms of the energy and the impact parameters according to the well-known equation[6]

$$e = [1 + (K\dot{s}^2B)^2]^{1/2} \quad (9)$$

where K is a constant. Differentiating and then expanding Eq. (9) in powers of $1/e$, one obtains to the first order $\Delta e = 2e\Delta\dot{s}/\dot{s} + e\Delta B/B$. Combining with Eq. (8) one obtains $\Delta B/B \sim -4\Delta\dot{s}/\dot{s}$. Again, by use of the value $\Delta\dot{s} = 10^{-2}$ km/sec, the preceding equation predicts $\Delta B = 40$ km. This is reasonably good agreement with the orbit determination program results in Table 4 of errors in B which range from 1 to 10 km.

An examination of the various orbit determination solutions using simulated data suggest the following conclusions: 1) All data perturbed by an acceleration that the orbit determination program cannot approximate with "solve for" accelera-

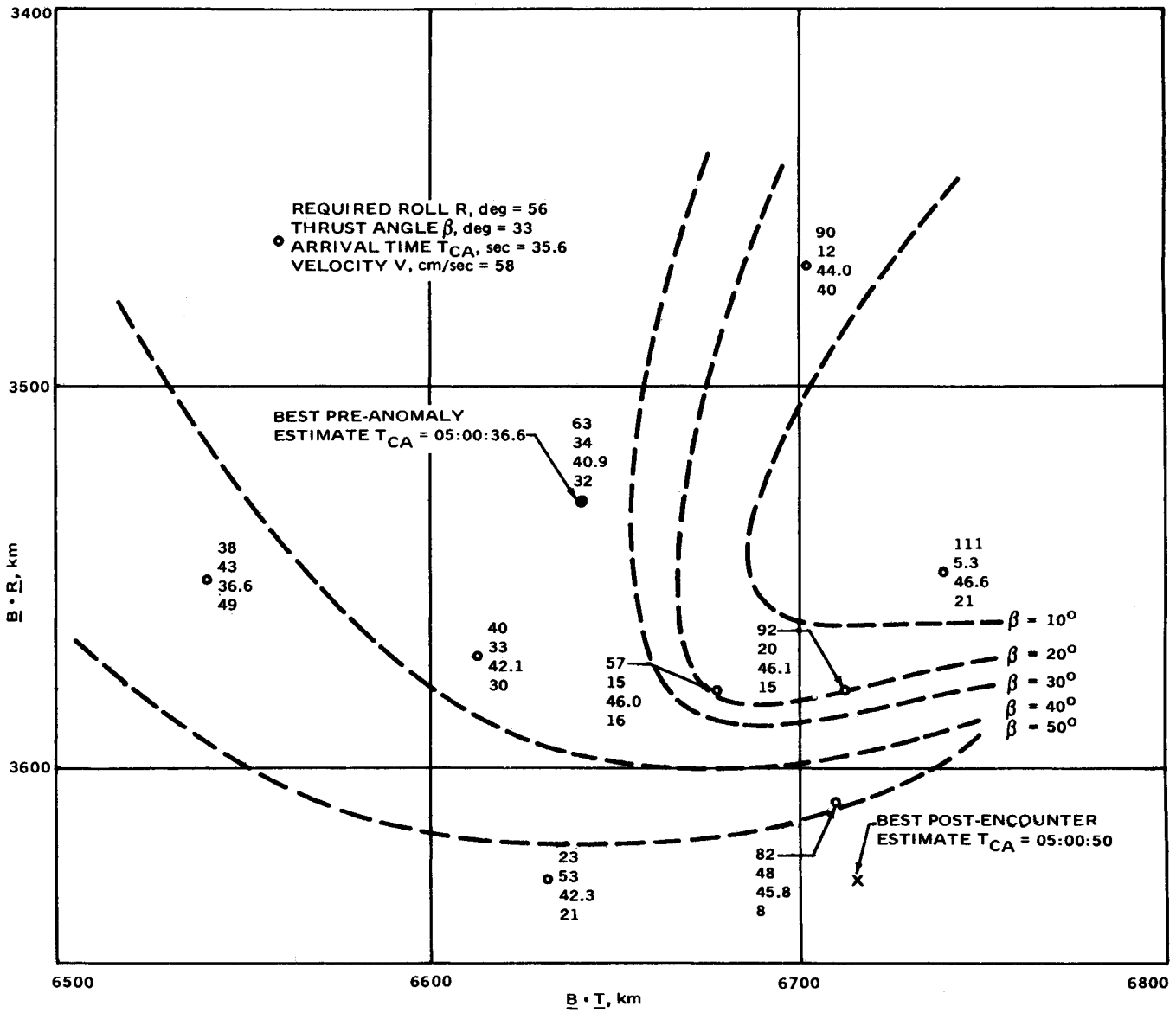

Fig. 10 Contours of equal β.

tions should be deleted. 2) The inclusion of encounter and postencounter data should allow the determination of the B-plane parameters to within 10 or 15 km for perturbations of the type experienced by Mariner VII.

Conclusions

Telemetry showed unexpected battery charger fluctuations starting approximately four days before the anomaly. It is assumed that a battery failure occurred and internal pressure began building up. This caused the battery case to rupture and vent into the spacecraft interior, causing a series of corona discharges across the Canopus star tracker power supply, which appeared to be a loss of Canopus, initiating a roll search and moving the high-gain antenna away from the Earth direction. Subsequent venting through openings in the thermal blanket caused small particles to break loose as well as imparting the observed translational acceleration. The particles near the spacecraft reflected sunlight into the Canopus star tracker and terminated the roll search. As the battery continued venting, the opening was cooled enough to freeze over and seal the assumed hair-line crack. This was the configuration of the spacecraft when low-gain antenna transmission was commanded and the signal was reacquired. The second LOS was caused by a similar set of circumstances after the battery case had warmed up enough to reopen the hair-line crack, which never froze over again as the internal pressure and venting rate were much lower than initially.

The uncertainties in the preanomaly orbit estimates are considerably greater than those in the postencounter estimates. Figure 8 shows these estimates, with their $1 - \sigma$ uncertainties mapped to the B-plane. In order to determine what the actual change in B-plane position was, the effective thrust direction due to escaping gas may be considered to consist of a component normal to Bay 2, which had the largest open area, and a component along the roll axis defined by the angle β in Fig. 9. A three-dimensional surface of possible preanomaly orbits may be constructed, characterized by four parameters: roll angle R, thrust angle β, unperturbed arrival time T_{CA}, and velocity change V. Figure 10 shows several contours of equal thrust angle β. Since β should be a small angle, and since the velocity change due to the venting of one battery monoblock should be on the order of 12 cm/sec, the actual preanomaly orbit would have been in the lower right side of the plot. This is consistent with the roll angle position of 73° from normal cruise orientation at the time of reacquisition of signal (as determined by the time necessary to acquire Canopus when a roll search was commanded). The actual trajectory change was therefore quite small, but the attempt to fit the data containing nongravitational acceleration greatly distorted the orbit as explained by the attempt to fit the simulated data which were generated to study this effect.

References

[1] Anderson, J. D., "Trajectory Determination From Observational Data," *Science and Technology*, Vol. 9, American Astronautical Society, 1966, pp. 133–158.

[2] Warner, M. R. and Nead, M. W., "SPODP—Single Precision Orbit Determination Program," TM 33-204, Feb. 15, 1965, Jet Propulsion Lab., Pasadena, Calif.

[3] Warner, M. R., Nead, M. W., and Hudson, R. H., "The Orbit Determination Program of The Jet Propulsion Laboratory," TM 33-168, March 18, 1964, Jet Propulsion Lab., Pasadena, Calif.

[4] Kizner, W. A., "A Method of Describing Miss Distances for Lunar and Interplanetary Trajectories," External Publication 674, Aug. 1, 1959, Jet Propulsion Lab., Pasadena, Calif.

[5] Mulhall, B. D. and Wimberly, R. N., "Conversion of Ionospheric Measurements to Doppler Correction for Deep Space Probe Tracking Data," *Supporting Research and Advanced Development*, Space Programs Summary 37-55, Vol. II, Jet Propulsion Lab., Pasadena, Calif., Jan. 31, 1969, pp. 19–22.

[6] Curkendall, D. W. and McReynolds, S. R., "A Simplified Approach for Determining the Information Content of Radio Tracking Data," *Journal of Spacecraft and Rockets*, Vol. 6, No. 5, May 1969, pp. 520–525.

[7] Goldstein, H., *Classical Mechanics*, Addison-Wesley, Redding, Mass., 1959.